

REPLACING DIESEL-DRIVEN GENERATORS WITH BATTERIES TO POWER ISLANDED GRIDS: MODELING AND PERFORMANCE COMPARISON

Claudia BERNECKER-CASTRO¹, Johanna TIMMERMANN¹, Rolf WITZMANN¹,
Tobias LECHNER², Sebastian SEIFRIED², Michael FINKEL², Kathrin
SCHAARSCHMIDT³, Steffen HERRMANN⁴

¹ Technical University of Munich, Chair of Electric Power Transmission and Distribution, Arcisstraße 21, D-80333 München, 0049 89 289-25098, claudia.bernecker-castro@tum.de, www.een.ei.tum.de

² Technische Hochschule Augsburg, Faculty of Electrical Engineering, An der Hochschule 1, D-86161 Augsburg, www.tha.de

³ LEW Verteilnetz (LVN) GmbH, Schaezlerstraße 3, D-86150 Augsburg, www.lew-verteilnetz.de

⁴ AVS Aggregatebau, Salemstraße 43, D-89584 Ehingen-Stetten, www.avs-aggregatebau.de

Abstract: During scheduled maintenance, grid operators use low- to medium-sized mobile generators to continue providing electricity during power interruptions. Internal combustion engines like diesel motors are frequently the prime mover in these field cases. By this, an intentional islanded grid is formed temporarily. To reduce the environmental impact of these use cases, a battery-generating unit can be used instead.

This paper presents the modeling and validation of a battery-generating unit using measurement data. Its performance against a diesel-driven mobile generator is analyzed for two different cases.

Results show that the frequency and voltage response of the replaced aggregate are several times faster than when using traditional mobile generators. The stable islanded operation may not be jeopardized since neither drop exceeds the normatively defined thresholds of decentralized generation (DEA).

Keywords: Diesel Generator, battery-generating unit, islanded grids, decentralized generation, dynamical modeling, grid-forming units

1 Introduction

It is well-known that to achieve carbon-neutral goals in the electricity sector, it is necessary to increase the penetration of feed-in power from renewable sources, e.g., solar and wind. This has changed the power grid structure and brought challenges to its stable operation. High penetration rates of inverter-based resources have raised questions, for example, regarding the amount of available short-circuit power and inertia on interconnected systems as well as in isolated grids. The dynamic interaction among multiple generators and types of load is also unknown.

The results shown in this paper are generated as part of the project LINDA 2.0. LINDA stands for (in German): Lokale (teil-) automatisierte Inselnetz- und Notversorgung mit dezentralen Erzeugungsanlagen bei großflächigen Stromausfällen). The project aims to investigate the feasibility of the formation and operation of electrically isolated grids as an emergency but sustainable solution in case of long-lasting blackouts. This is the case when no communication means, additional controllers, or even changes in the already installed protection systems, with respect to the grid-connected mode of operation, are considered.

During scheduled maintenance, parts of the electrical network are supplied by low to medium-sized generators like diesel engines. By this, an intentional and temporal islanded grid is formed. Usually, the generator is operated, so the power injection from installed decentralized generators (DG), such as rooftop PVs, is not allowed. However, a control strategy for a stable islanded grid operation using a mix of conventional generators together with DGs has been proposed [1] and successfully tested in the field [2].

The carbon footprint of such individual events can be further reduced by replacing these combustion engines with a battery-generating unit. The battery can be charged with the surplus electricity generated from decentralized generators available in the low-voltage network and discharged when the demand increases. As described in [3], a small diesel-driven generator is included in this concept and designed for times when the battery needs to be recharged. This functionality is also known in the literature as a range extender. By this, the state of charge of the battery does not fall below the minimum defined by the manufacturer, which could compromise the stable islanded operation.

This paper describes the modeling of the diesel generator and the battery-generating unit, which are intended to be used as the grid-forming units during islanded operation. The controller parameters were validated using measurement data from a test setup for both generator cases. In addition, their frequency and voltage performance under two worst-case load step scenarios are compared.

2 Model Description and Validation

Both grid-forming units were modeled using DIgSILENT Power Factory 2022 [4]. The network configuration consisted of the generating unit connected to a load. For the model validation, 10 ms RMS measurement data from different load steps and base loads were considered. This section describes all the components of both grid-forming units.

2.1 Diesel generator

The three-phase diesel-driven generator used for the project LINDA 2.0 has characteristics described below. (in German: Netzersatzaggregat and shortened in the rest of this work as NEA)

Synchronous Generator:

- Rated Power: 300 kVA (240 kW)
- Rated Voltage: 400 V

Engine:

- Speed: 1500 rpm

- Gross power: 253 kVA (226 kW)
- Working principle: 4-stroke

The model of the NEA comprises two standard controllers: IEEE EXAC1 and Woodward DEGOV, as shown in Figure 1a). The corresponding parameters were identified after performing several load steps under different pre-loading conditions and are considered in this work for the performance comparison. The methodology and results are detailed and described in [5].

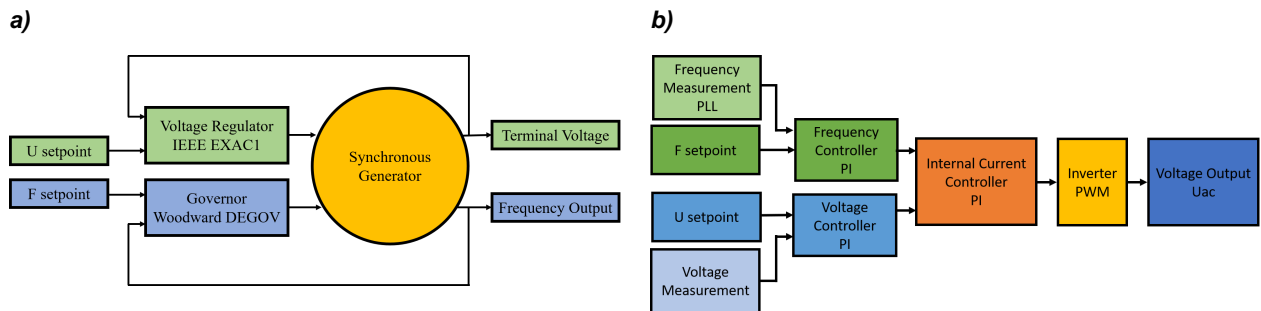


Figure 1: Comparison between the model of the a) diesel-electric generator and b) battery-generating unit

2.2 Battery-generating unit

The battery-generating unit used for the project LINDA 2.0 comprises the following elements: a Li-Ion battery, an inverter, a filter, and a transformer, as described below:

Battery:

- Chemistry: Li-Ion NMC (180 Cells in Total)
- Capacity: 600 Ah
- Number of Battery Systems: 12 Battery Systems of 50 Ah each, connected in parallel
- Nominal voltage: 655 V

Inverter:

- DC link nominal voltage: 750 Vdc
- Maximum power: 300kW, $I_{max} = 350$ Arms
- AC output voltage: 0-560 Veff ($U_{dc} = 800$ Vdc)

Filter:

- Inductance: 0.20 mH

Transformer:

- Power: 300 kVA
- Output: 3x 400 V
- Switch group: Dyn5
- Frequency: 50/60 Hz

The battery-generating unit model includes a detailed model of the Li-Ion Battery as well as the inverter, in addition to the other components mentioned above, as shown in Figure 2.

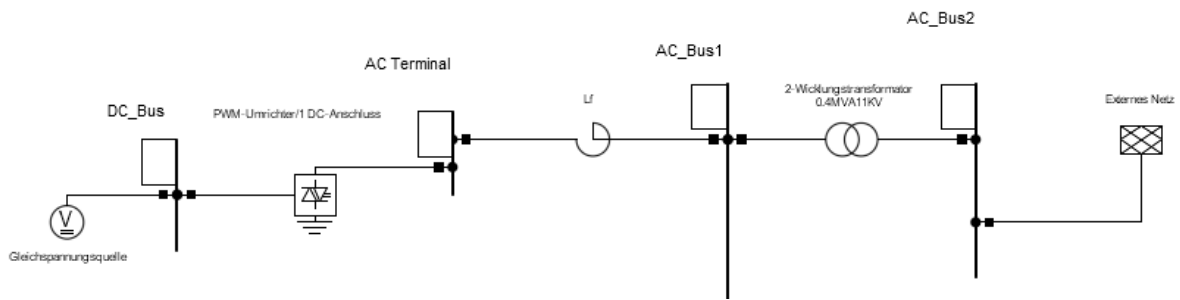


Figure 2 Grid Schematic of the battery-generating unit model

The Battery model considers the dependency between the open circuit voltage (OCV) and the state of charge (SoC), as well as the resistive and capacitive characteristics associated with the cell chemistry (Li-Ion NMC).

The resultant DC Voltage was measured for a region where the state of charge lay between 60-80%. Figure 3 shows a comparison between the resultant DC-Voltage for standard Li-Ion NMC batteries [6] (orange) versus measurement data from two field tests. The measurement of Test 1 (blue) corresponds to several load steps when the battery was in the discharging mode of operation. The measurement of Test 2 (grey) corresponds to several load steps when the battery changed between the charging and discharging modes.

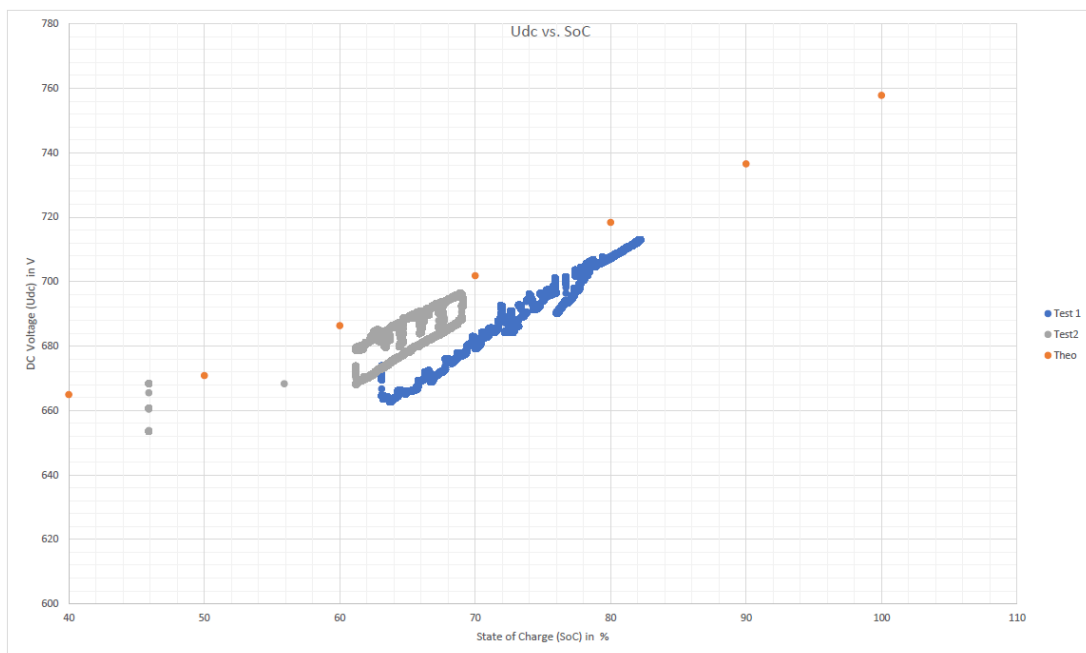


Figure 3 Open Circuit Voltage (OCV) versus State of Charge

Figure 3 shows that the DC voltage can be slightly different depending on the mode of operation. The difference between the OCV and measured DC Bus voltage can be attributed to the cell resistance.

Within the scope of this work, no effects due to the variation of the DC Voltage on the AC Output were identified from the field tests or the simulation, as described in section 3. Nonetheless, a voltage drop below the manufacturer-defined level can shorten the battery's lifetime. On the other side, overvoltage can threaten the safe operation of the battery system

[7]. Detailed modeling of these effects is difficult to validate with the available system and is outside the scope of the research project.

The inverter model is composed of external and internal controllers that regulate the behavior of the PWM block, both modeled as two separate proportional-integral (PI) controllers, as shown in Figure 1b). The external controller regulates the setpoint of frequency and voltage in islanded operation. The inverter has the ability to work in parallel mode by regulating the active and reactive power instead. In this work, only the external controllers were validated, that is, for the regulation of frequency and voltage regulation.

As [8] explains, the external controllers output a reference for the current's direct I_{d_ref} and quadrature I_{q_ref} components. The internal current regulates the difference between the reference and measured inverter current and calculates the modulation index m_d and m_q , which is necessary to form the voltage output.

The PWM block calculates the terminal voltage of the block based on the modulation methods, the modulation index, and the DC link voltage. These mathematical operations are performed in the $\alpha\beta$ -frames (Park transformation is internally implemented).

The controller parameters for voltage and frequency were validated using measurement data from a test setup composed of a resistive load bank connected to the output of the battery-generating unit. Different base loads and load steps on the discharging mode of operation were recorded. Although the parameters were identified for a base load of 50 kW and a load step of approx. 200 kW, the same values are also valid for measurement sets with different base loads and load steps, as shown in Table 1.

Given that each PI controller is composed of a proportional gain (k_p) and an integral gain (k_i) a total of 8 controller parameters were identified for the complete model of the battery-generating unit. The internal current controller parameters (k_d, k_i, T_d, T_a) were identified first, having stronger integral gains than the external controllers i.e. the internal controller is faster than the external controller. After this, the proportional (K_{fp}) and integral (K_{fi}) gains of the frequency controller were identified. Then, the voltage controller parameters (K_v, T_v) were identified. At the end, the frequency controller parameters had to be slightly updated, giving the final set of values.

During field tests, it was observed that the worst performance of both generating units happens when power jumps should be performed starting from idle. Longer time constants, deeper nadir frequencies, and a marked unsymmetrical behavior were observed. The results from the validated model and measurement data will be compared for load steps under the two conditions: unloaded (from idle) and for a base load of 50 kW. The results for the frequency and voltage output for the battery-generating unit are shown in Figure 4 and 5.

Figure 4 shows a comparison among the measurement and simulation curves for the validated model. The measurement data corresponded to the device operating in idle mode, and a load step was performed at $t = 10$ s. The blue and green curves show a load step of 50 kW and 100 kW, respectively. Similarly, Figure 5 corresponds to a base load of 50 kW and the same load steps as in Figure 4.

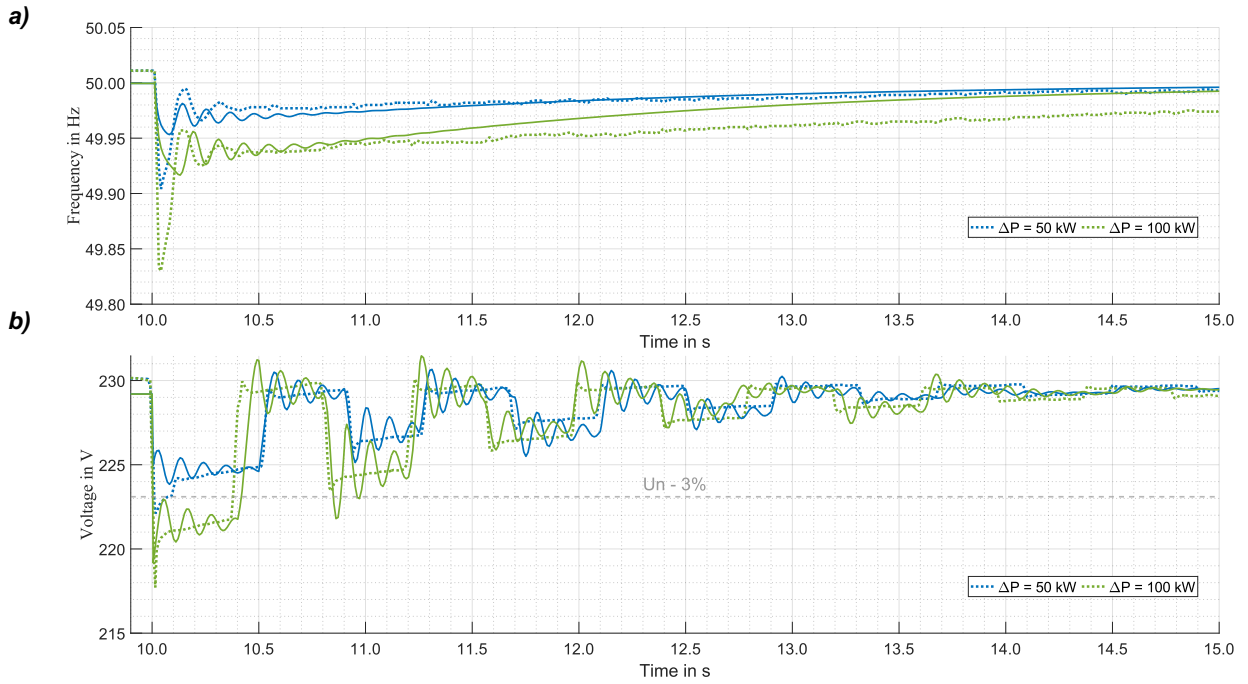


Figure 4: Comparison of the measurement and simulation values for a base load of 0 kW (idle) and two load steps for a) frequency and b) voltage response

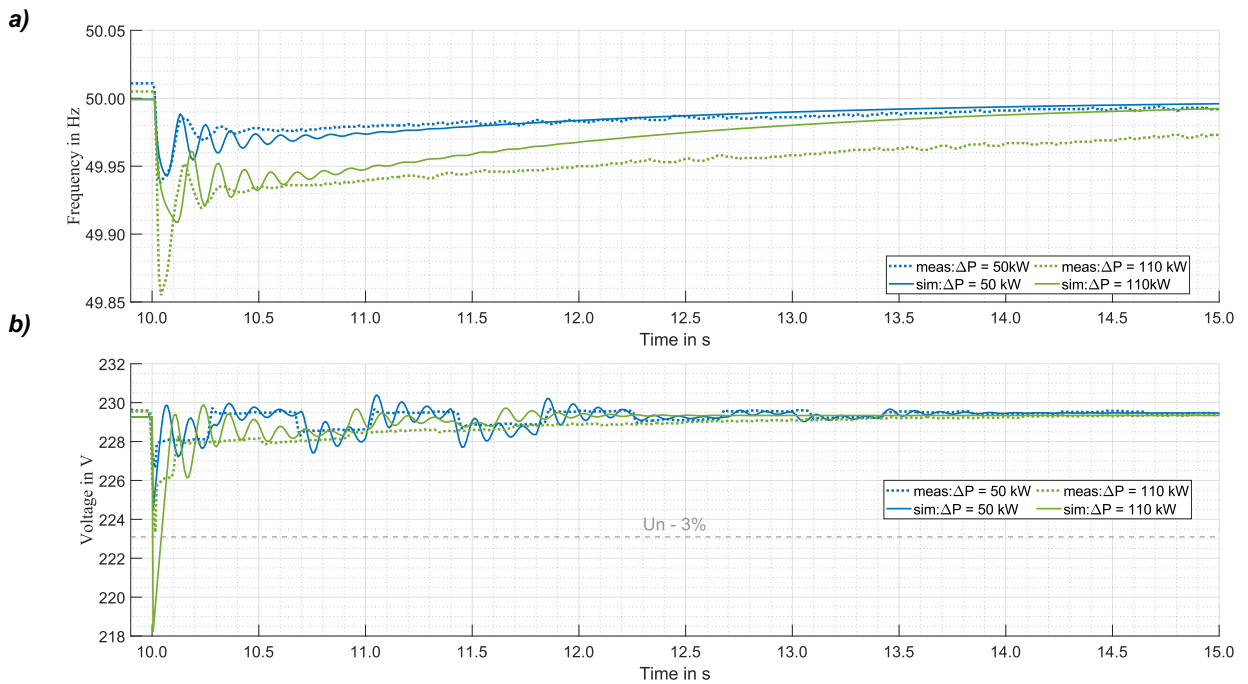


Figure 5: Comparison of the measurement and simulation values for a base load of 50 kW and two load steps for a) frequency and b) voltage response

From Figure 4 and Figure 5, it can be observed that the frequency and voltage outputs have deeper minimums for higher load steps. As previously described, longer time constants were observed for a load step of 100 kW than for 50 kW. These effects are also replicated by the validated simulation model.

Additionally, the voltage output oscillates between values that tend towards the nominal voltage value (stair behavior). This can be explained by the existence of an internal voltage

droop, which is applied every time a load step is observed on the inverter and whose setpoint is updated approximately every 500 ms. The differences from the nominal value on the voltage output can be attributed to the data format of the setpoint sent by the controller to the inverter. Nevertheless, the precision of the setpoint values is unknown.

When a decentralized generator (DG) is to be connected to a low-voltage grid, it should follow the behavior described in the German standard VDE 4105 [9]. According to this norm, the maximum voltage change allowed for DGs (with respect to the case without DGs) is 3 %. Considering the network quality criteria according to EN 50160, this limit is 5% for fast voltage changes. In this work, the limit defined by the VDE 4105 was considered to evaluate the aggregate's performance. Thus, it is also identified in the voltage graphs. It can be observed that only in the case of idle and a load step of 100 kW does the voltage output response fall outside the 3 % limitation. This can be avoided when the battery-generating unit is previously loaded, e.g., 50 kW (Figure 5).

To evaluate the validated model's reliability, the error between the recorded measurement and simulation for the nadir frequency (f_{nadir}), rate of change of frequency after 40 ms (RoCoF) and the minimum voltage (V_{min}) was calculated. Table 1 shows an overview of the defined errors ε , for the cases presented in this work. The validated simulation model is considered to be acceptable when the error in the f_{nadir} prediction is a maximum of 200 mHz away from the real measurement data. No similar condition is defined for the RoCoF or voltage response evaluation.

Table 1: Overview of errors in the frequency prediction of the validated model for the Battery-generating unit for selected cases

Base Load in kW	Load step in kW	ε_{fnadir} (mHz)	ε_{RoCoF} (Hz/s)	ε_{Vmin} (V)
0 (idle)	50	49.2	0.316	1.730
0 (idle)	100	86.6	0.339	1.476
0 (idle)	200	86.7	0.292	9.775
50	50	4.9	0.302	3.356
50	110	53.7	0.184	5.141

From Table 1, it can be noticed that the validated model has an acceptable performance for the frequency response since in all the cases $\varepsilon_{fnadir} \leq 200$ mHz.

For a similar load change of 50 kW, it can be expected a prediction error of 4.9 mHz for the case when a base load of 50 kW is applied meanwhile it is expected a prediction error of 49.2 mHz for idle, that is, up to 10 times higher prediction error is expected for the idle condition than a previously loaded aggregate.

The ε_{RoCoF} column shows that there is an error in the prediction of the validated model with respect to the measurement data in the order of mHz per second for all the cases.

Since no condition for the voltage evaluation has been defined, it is difficult to evaluate the acceptability level of the validated model for the voltage output. However, it can be stated that

the current parameters have improvement potential for the higher load steps since an error of up to 9.7 V for a load step of 200 kW from idle was recorded.

3 Performance Comparison

Field test measurement data show that power jumps on low-voltage grids typically range from 10 to 50 kW and up to 100 kW within a few seconds during changeable weather. This statement is valid for the low-voltage networks, where the concept LINDA was tested.

As previously stated, the generating unit's worst performance condition was identified at a base load of 0 kW (idle). This section presents a performance comparison between the NEA and the battery-generating unit. The first analysis considers a worst-case scenario for a low-voltage (LV) network when both units start at idle. The second analysis considers a load profile as defined in the ISO 8528 [10].

Analysis 1: A worst-case load step in a LV Network

The performance comparison between of the NEA to the battery-generating unit for a change from idle to 50 kW is shown in Figure 6. The NEA performance is shown in blue; meanwhile, the battery-generating unit is in green. Both measurement and simulation data are illustrated.

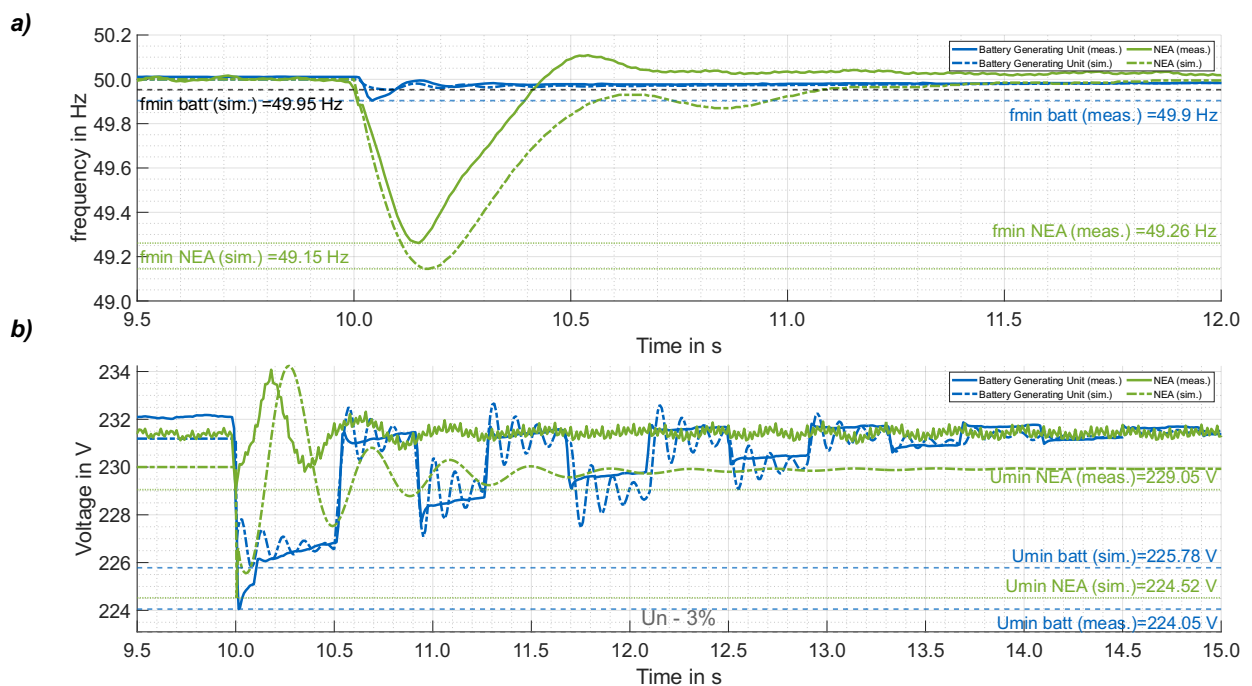


Figure 6: Comparison of idle to 50 kW performance among the NEA and the battery-generating unit for a) frequency and b) voltage response.

From Figure 6, it can be noticed that the difference in the measured minimum frequency between both devices lies around 650 mHz. It can also be observed that the reaction time of the battery-generating unit takes around 200 ms; meanwhile, the diesel generator returns to the setpoint after a few seconds.

Similarly, the difference in the measured minimum voltage between both devices lies around 5.0 V. It can also be observed that the reaction time of the battery-generating unit is slightly longer than for the NEA, approximately within 1-2 s and one second, respectively.

Nevertheless, the voltage response for both aggregates was above the defined limit of 3% from the nominal voltage.

The protection systems' configuration of the DEAs is defined by the connection norms for grid-connected behavior [9]. In the case of (LV) German electrical networks, an uncritical operation range in grid-connected mode, the frequency is between 47,5 Hz and 51,5 Hz; meanwhile, the voltage is inside the $0.8 - 1.10 U_n$ range. Since both NEA and battery-generating unit output behaviors (frequency and voltage) are located inside the normative limits, it is not expected that the investigated case will cause the disconnection of DEAs and, thus, will not jeopardize the islanded grid operation.

Analysis 2: A worst-case load step scenario according to ISO8528

According to ISO8528-5 [10], the performance of a generating set with a reciprocating internal combustion engine can be classified into four categories: G1, G2, G3, and G4. The G1 performance class has the broadest allowed deviation from the nominal values for frequency and voltage performance, and G3 has the smallest. An engine with performance class G4 has performance defined by an agreement between the manufacturer and the customer. The performance class is evaluated according to a load profile defined by the break mean pressure of the engine [11]. For the characteristics of the NEA as part of the project LINDA 2.0, the evaluating load profile should perform load steps illustrated in Figure 7. The validated models performed a similar evaluating load profile for the NEA as well as the battery-generating unit.

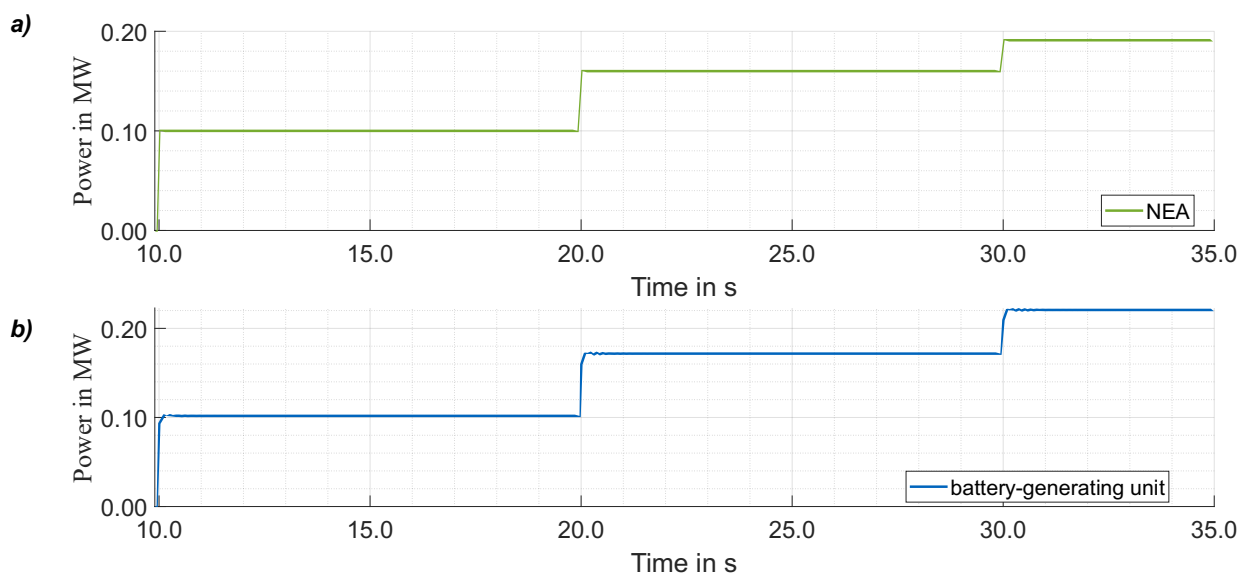


Figure 7: Evaluating load profile according to ISO8528-5 for the a) NEA and b) battery-generating unit

Figure 8 shows the results of a simulative comparison between the performance of the NEA (with blue) and the battery-generating unit for the same evaluating load profile, as previously described. It is evident that the f_{nadir} and reaction times for the battery-generating unit are significantly smaller than for the NEA. Similar performance can be observed for the voltage case i.e. smaller voltage depths and faster recovery times. For simulation purposes, the droop on the voltage controller was deactivated.

Therefore, a better output performance can be achieved by replacing the diesel generators with a battery generating unit.

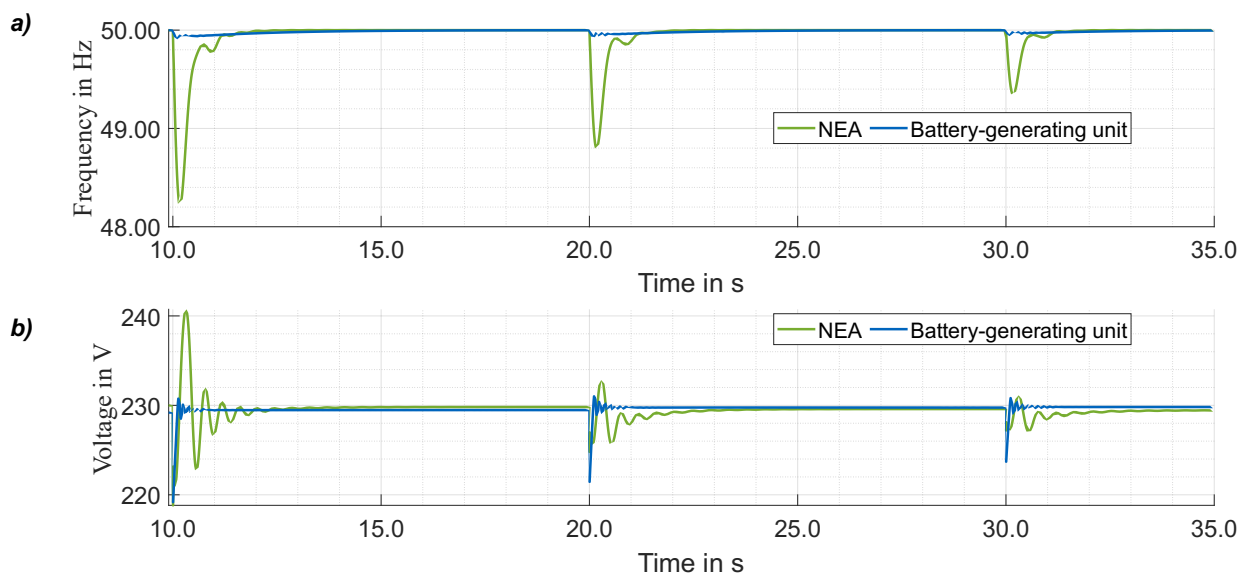


Figure 8: Performance comparison between NEA and battery-generating unit (simulated) for the evaluating load profile

However, output behavior is only one characteristic to consider when replacing diesel-driven mobile generators with battery-based aggregates to power islanded grids. Additional aspects should be further explored, like the availability of enough short-circuit power, black-start capability, control parameters for different constellations of islanded grids and interactions between inverters and NEAs.

Analysis 3: DC Side modeling

Figure 9 illustrates a simulation of the frequency and voltage output for the same evaluating load profile as in Analysis 2. The results from including the battery model at a SoC = 80% and SoC=20% are compared to the case without a battery model. There is no noticeable effect on the output (frequency nor voltage) due to the change in the starting SoC.

Nevertheless, the effects on the DC-bus are noticeable, as shown in Figure 10.

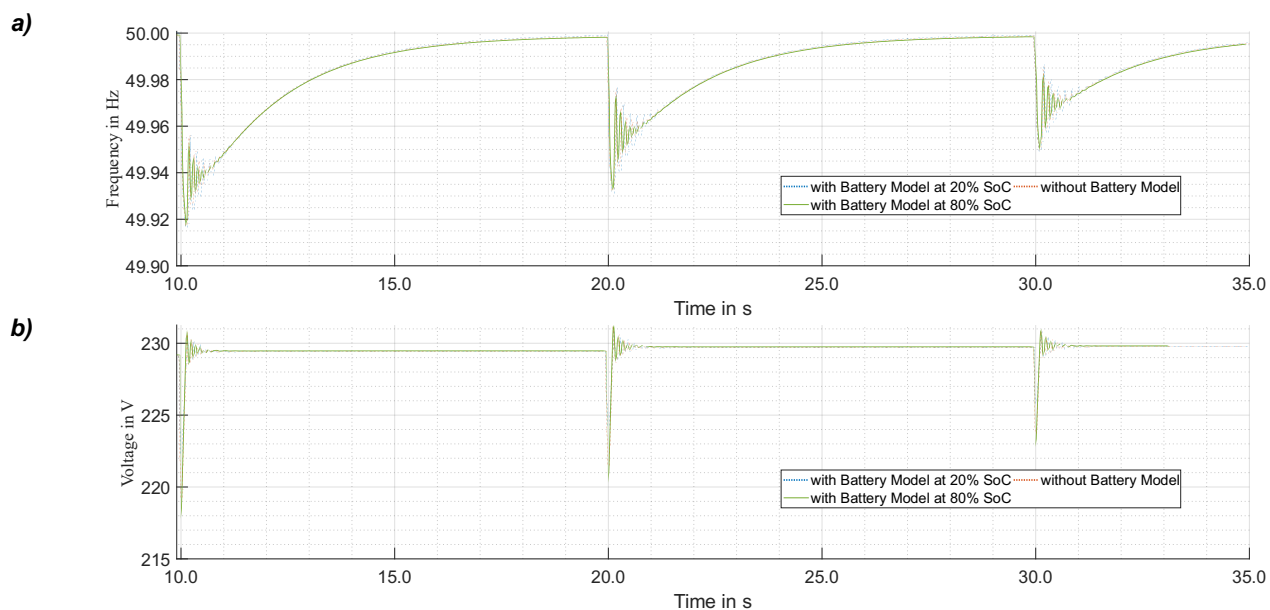


Figure 9: Frequency and voltage output of the battery-generating unit for the evaluating load profile

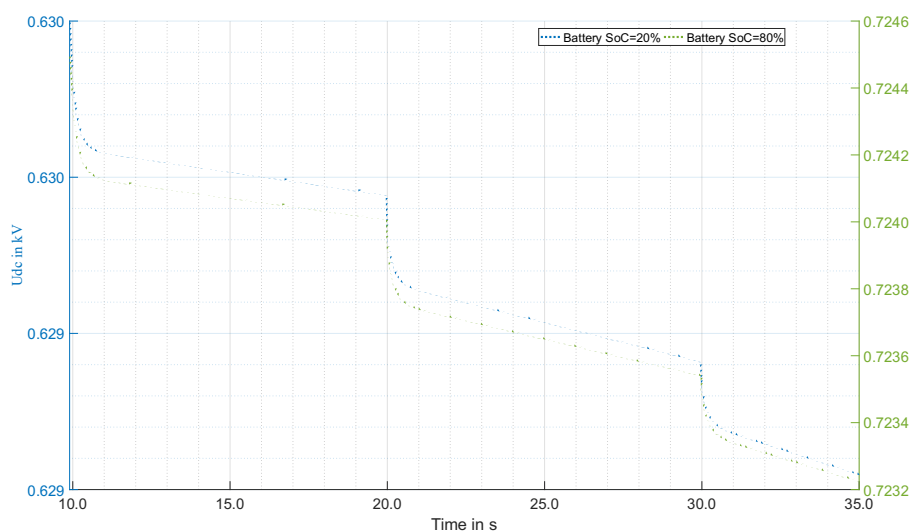


Figure 10: DC-Bus Voltage development for the evaluating load profile for a starting SoC = 20% (blue) and SoC = 80% (green)

4 Conclusion and Future Scope

A model of a battery-generating unit was built and validated using measurement data. The standard inverter model in DlgSILENT Power Factory was parametrized according to the manufacturer's datasheet. The controller parameters were validated using one set of measurement data inside the discharging operation region. The same parameters are considered to be valid for other test cases since the simulation results for the f_{nadir} are maximum $\varepsilon=200$ mHz away from the measurement data.

The performance of a battery-generating unit is better than a diesel-electric generator in terms of voltage and frequency output. This paper analyzed a typical use case of a power jump from idle to 50 kW and an evaluating load profile as defined in [11]. Nevertheless, other aspects

should be additionally researched, such as synchronization behavior, black start capability, and short-circuit behavior.

According to the measurement data and simulation, the inverter output is not compromised due to overvoltage or undervoltage on the DC Side. The safety aspects of the use of Li-Ion batteries are out of the scope of this work.

The validation of a model is an iterative process, which permanently receives new measurement data to update the controller values. It is expected to extend the validated region of the battery-generating unit model with measurements from load steps in the charging mode of operation as well as from sudden operation mode changes (from charging to discharging and vice versa).

The performance comparison of additional grid-forming units can be evaluated using the available validated models. The selection of the most suitable generating units for islanded grid operation might be dependent on the island grid configuration (generators and loads to be supplied).

The current validated model can be used to evaluate the current control strategy of islanded grids used in LINDA 2.0 [12] by means of dynamic simulation. By this, adequate time constants as well as control gains can be suggested.

5 References

- [1] G. Kerber, M. Finkel, K. Schaarschmidt, C. Steinhart, M. Gratza, R. Witzmann, „Konzept für eine lokale Inselnetzversorgung mit dezentralen Erzeugungsanlagen bei großflächigen Stromausfällen“, 14. Symposium Energieinnovation TU Graz, Graz, 2016
- [2] C. Steinhart et al., „Abschlussbericht zum Verbundvorhaben LINDA: Lokale Inselnetzversorgung und beschleunigter Netzwiederaufbau mit dezentralen Erzeugungsanlagen bei großflächigen Stromausfällen“, 2019.
- [3] T. Lechner et al. “Betrieb von hybriden Netzersatzanlagen mit der Einbindung von dezentralen Erzeugungsanlagen und die daraus resultierenden Fragstellungen zum EEG”, 13. Internationale Energiewirtschaftstagung IEWT, Wien, 2023
- [4] „DigSILENT Power Factory Solutions,“ DigSILENT, [Online]. Available: <https://www.digsilent.de/de/home.html>. [Zugriff am 04 02 2024].
- [5] C. Bernecker-Castro et al., „Methodology for identification of controller parameters of a diesel generator in islanded grid operation “, Conference on Sustainable Energy Supply and Energy Storage Systems (NEIS), Hamburg, 2023
- [6] M. Than, A. DaCosta, A. Mevawalla, S. Panchal, M. Fowler, “Comparative Study of Equivalent Circuit Models Performance in Four Common Lithium-Ion Batteries: LFP, NMC, LMO, NCA”, Batteries 2021, 7, 51, <https://doi.org/10.3390/batteries7030051>
- [7] S. R. (Jauch), „What actually happens when lithium batteries are overcharges or deep discharged?“, [Online]. Available: <https://www.jauch.com/blog/en/what-actually-happens-when-lithium-batteries-are-over-charged-or-deep-discharged/>. [Zugriff am 04 02 2024].
- [8] P. Pachanapan, “Dynamic Modelling and Simulation of Power Electronic Converter in DigSILENT Simulation Language (DSL): Islanding Operation of Microgrid System with Multi-Energy Sources”, Modelling and Simulation of Power Electronic Converter Dominated Power Systems in PowerFactory, pp.67-93, 2021

- [9] Verband der Elektrotechnik, Elektronik und Informationstechnik, VDE-AR-N 4105 „Technische Mindestanforderungen für Anschluss und Parallelbetrieb von Erzeugungsanlagen am Niederspannungsnetz“, Nov. 2018
- [10] ISO8528-5:2018 (E) Reciprocating internal combustion engine driven alternating current generating sets – Part 5: Generating sets
- [11] P. Ponte, “Transient Performance of Generating Sets”, Technical Information from Cummins, Web Address: <https://mart.cummins.com/imagelibrary/data/assetfiles/0058629.pdf> (04.02.2024)
- [12] T. Lechner et al., „Frequency Droop Characteristic for Grid Forming Battery Inverters – Operation in Islanded Grids with the Infeed of Distributed Generation Systems“, CIRED International Conference on Electricity Distribution, Rome 2023
- [13] M. Nuhic and G. Yang, “Battery Energy Storage System Modelling in DIgSILENT PowerFactory”, Modelling and Simulation of Power Electronic Converter Dominated Power Systems in PowerFactory, pp.177-200, 2021



Gefördert durch:



aufgrund eines Beschlusses
des Deutschen Bundestages